ANN Model For SiGe HBTs Constructed From Time-Domain Large-Signal Measurements

D. Schreurs, S. Vandenberghe, H. Taher, and B. Nauwelaers

K.U.Leuven, Div. ESAT-TELEMIC, Kasteelpark Arenberg 10, B-3001 Leuven, Belgium
e-mail: Dominique.Schreurs@esat.kuleuven.ac.be

We construct a large-signal artificial neural network (ANN) model for SiGe HBTs, directly from time-domain large-signal measurements. It is known that HBTs are very sensitive to self-heating and therefore we explicitly study the effect on the model accuracy of the incorporation of the self-heating effect in the behavioural model description. Finally, we show that this type of models can be accurate at extreme operating conditions, where classical compact models start to fail.

INTRODUCTION

Large-signal models for microwave devices are classically derived using small-signal information, being multi-bias S-parameter measurements. Due to recent advances in the metrology of *vectorial large-signal* measurements (1)-(4), several novel modelling methodologies circumventing this small-signal detour are being developed. Some examples of such modelling techniques include parametric equivalent-circuit model extraction (5)-(7), and behavioural model identifications in the frequency domain (7)-(8). We recently proposed a procedure to construct a *time-domain* behavioural model (9), where we built upon techniques developed in non-linear time-series analysis (NLTSA) (10).
Until now, this method has been demonstrated on diodes, HEMTs, and simple amplifier circuits. In this work, we apply the underlying methodology to construct a behavioural model for SiGe HBTs. In contrary to the previously studied devices, self-heating can no longer be neglected, and therefore we especially pay attention to the importance of including this effect in the model desciption.

In the following section, we describe the construction of the behavioural model. We first briefly review the principle of the method, and consequently provide details of the actual modelling procedure. As model representation form, we choose to adopt an Artificial Neural Network (ANN). Next, we present large-signal experimental results, and show how metrics could be used to quantitatively represent model accuracies. Finally, conclusions are drawn.

ANN MODEL CONSTRUCTION

Modelling method

The basic principle of the modelling method involves that the considered two-port microwave devices can be described by equations of the form:

$$\begin{aligned} I_1(t) &= f_1\left(V_1(t), V_2(t), \dot{V}_1(t), \dot{V}_2(t), \ddot{V}_1(t), \ddot{V}_2(t), \cdots, \dot{I}_1(t), \dot{I}_2(t), \cdots\right) \\ I_2(t) &= f_2\left(V_1(t), V_2(t), \dot{V}_1(t), \dot{V}_2(t), \ddot{V}_1(t), \ddot{V}_2(t), \cdots, \dot{I}_1(t), \dot{I}_2(t), \cdots\right) \end{aligned} \quad (1)$$

with $I_1(t)$ and $I_2(t)$ the terminal currents, $V_1(t)$ and $V_2(t)$ the terminal voltages, and the superscript dots representing the (higher order) time derivatives.

The objective of the modelling technique is to find the number of independent or state variables, and consequently to determine the functional relationships $f_1(.)$ and $f_2(.)$ by fitting the measured terminal currents to the measured state variables.

Modelling procedure

The model is built from time domain data, obtained by performing vectorial large-signal measurements using the Non-linear Network Measurement System (NNMS) (4). At the start of the modelling process, operating bounds for the model are established by defining the minimum and maximum values of the state variables. These bounds define the operating region within the state space for which the model is to be developed and used. To enable practical identification of the device dynamics, the measured time domain data need to sample this operating

region efficiently. For the considered SiGe HBTs, we fixed the fundamental frequency to 1.8 GHz and performed measurements at various input powers (ranging between –14 dBm and –4 dBm) and DC bias conditions. The operating range of interest is from 0.4 V to 1.2 V for the base-emitter voltage V_{be}, and from 0.5 V to 1.5 V for the collector-emitter voltage V_{ce}. These measurements are consequently de-embedded, because our interest is to model the device as if it will be inserted in an actual circuit design (hence, without the pads and access transmission lines).

The next step is to determine the independent (or state) variables. This can be accomplished by applying the "embedding" technique, based on the "false nearest neighbour" principle (11). Alternatively, one can deduce from the known physics of an HBT, that the dominant independent variables are the terminal voltages, as well as the corresponding first and second order time derivatives.

Consequently, the functional relationships $f_1(.)$ and $f_2(.)$ have to be determined by fitting the measured time domain terminal currents towards the measured independent variables. In Ref. (9), multivariate polynomials were used to describe $f_1(.)$ and $f_2(.)$. Polynomials however have known disadvantages, such as that higher-order polynomials have exponential-like asymptotes, which might give cause to convergence problems. Therefore, we explore the use of artificial neural networks (ANNs) in this work, whereby the activation function is the sigmoid function, which has smooth limits. For this particular case, we use an artificial neural network with 6 inputs (the voltages up to the second derivative) and two outputs (the currents). The ANN is trained using the back-propagation algorithm, as implemented in the Neuro-modeler program, which is described in detail in Refs. (12)-(14).

We found that an ANN with a single hidden layer of 28 neurons provides the best trade-off between model accuracy and model complexity. Table 1 summarizes the training results, consisting of the average and maximal training errors for both currents. The table also lists the correlation coefficient, which is a measure for whether we selected the right set of independent variables. The correlation is rather good, but we notice that the maximal training errors are too large. The reason is that the device is very temperature dependent, and this effect has not been incorporated yet in the model description.

To properly account for self-heating, we add a 7th independent variable, being the net dissipated power: P_{dc}*(1-PAE) (15)-(16). The corresponding training results are also listed in Table 1 (case 2). We notice the clear improvement in terms of both correlation and training errors. The high correlation indicates that we now have the right set of independent variables.

Finally, we also train an ANN based on non-de-embedded data. The results (case 3 in Table 1) deteriorate slightly compared to case 2. The reason is that a second order time derivative might no longer be sufficient to represent the distributed behaviour of the access transmission lines.

LARGE-SIGNAL EXPERIMENTAL RESULTS

We implement the time-domain behavioural model corresponding to case 2 in the Agilent ADS microwave circuit simulator by means of a symbolically defined device (SDD). The SDD can calculate the time-derivatives of the terminal voltages at each time-step in the simulation, enabling the fitting functions for the currents to be evaluated.

In Fig. 1, we compare measured and simulated time-domain waveforms of the terminal currents for 2 different experimental conditions (listed in the Caption). Condition 1 (top) corresponds to turn-on, whereas condition 2 (bottom) represents a high V_{be} case, which is often difficult to model by compact models. The simulations were carried out at exactly the same excitation conditions as the measurements. Based on these plots, we can conclude that a good model prediction can be obtained, providing the range of measurements used in the training process span all instantaneous conditions of the verification measurements.

This visual interpretation of the model accuracy can also be objectively quantified by the use of metrics. Table 2 lists the metric values for the scattered waves b_1 and b_2, corresponding to the two experimental conditions of Fig. 1. We consider two different formulations expressed in the frequency domain, being the natural metric and a weighted metric (17):

1. the natural metric

$$S(x,\hat{x}) = \left|x_0 - \hat{x}_0\right|^2 + 2\sum_{i=1}^{N}\left|x_i - \hat{x}_i\right|^2 \qquad (2)$$

2. a weighted metric

$$S(x,\hat{x}) = \left|x_0 - \hat{x}_0\right| + \sum_{i=1}^{N}\frac{\left|x_i\right|}{\sum_{j=1}^{N}\left|x_j\right|}\left|x_i - \hat{x}_i\right| \qquad (3)$$

The value S summarises the differences between modelled ($\hat{x}$) and measured (x) quantities, where i and j are harmonic indices, N is the number of harmonics considered, and the subscript 0 denotes the DC value. In the case of the natural metric, all finite-order harmonics are treated equally, so it is directly related to the corresponding differences in time-domain waveforms, whereas in the case of the weighted metric, errors in predicting the dominant harmonics have a relatively larger contribution to the overall metric value. Setting a preference for either of the metrics is not straightforward, as it depends on the model application. When the harmonics with a lower power level are as important as the high-power harmonics (e.g., in mixer applications), then the natural metric may be preferred.

From the metric results listed in Table 1, we can conclude that the accuracy in predicting b_1 is slightly better compared to that of b_2. Furthermore, the obtained accuracy is comparable for the two considered experimental conditions.

CONCLUSION

For the first time, we presented the construction of a behavioural model for SiGe HBTs from time-domain large-signal measurements. The self-heating effect is incorporated by an additional independent variable, being the dissipated power. The resulting small ANN training error and the good agreement with large-signal verification data show that we selected a good set of independent variables. Finally, we showed that the use of metrics has a surplus value compared to visual interpretations of experimental data, as model accuracy can be quantified by a number.

ACKNOWLEDGEMENT

D. Schreurs is supported by the Fund for Scientific Research-Flanders as a post-doctoral fellow. The authors acknowledge Alcatel Microelectronics for the SiGe HBT devices, and Agilent Technologies for the donation of the NNMS, as well as for the support to implement the behavioural models into ADS. The authors also thank Dr. D. Root, NIST and Prof. K.C. Gupta for the interesting discussions.

REFERENCES

(1) F. van Raay and G. Kompa, *"A new on-wafer large-signal waveform measurement system with 40 GHz harmonic bandwidth,"* IEEE MTT-S Int. Microwave Symp. Dig., pp. 1435-1438, 1992.

(2) M. Demmler, P. Tasker, and M. Schlechtweg, *"A vector corrected high power on-wafer measurement system with a frequency range for the higher harmonics up to 40 GHz,"* Proc. European Microwave Conference, pp. 1367-1372, 1994.

(3) C. Wei, Y. Lan, J. Hwang, W. Ho, and J. Higgins, *"Wave-form characterization of microwave power heterojunction bipolar transistors,"* IEEE MTT-S Int. Microwave Symp. Dig., pp. 1239-1242, 1995.

(4) J. Verspecht, P. Debie, A. Barel, and L. Martens, *"Accurate on wafer measurement of phase and amplitude of the spectral components of incident and scattered voltage waves at the signal ports of a nonlinear microwave device,"* IEEE MTT-S Int. Microwave Symp. Dig., pp. 1029-1032, 1995.

(5) D. Schreurs, J. Verspecht, B. Nauwelaers, A. Van de Capelle, and M. Van Rossum, *"Direct extraction of the non-linear model for two-port devices from vectorial non-linear network analyzer measurements,"* Proc. European Microwave Conference, pp. 921-926, 1997.

(6) M. Curras-Francos, P. Tasker, M. Fernandez-Barciela, Y. Campos-Roca, and E. Sanchez, *"Direct extraction of nonlinear FET Q-V functions from time domain large-signal measurements,"* IEEE Microwave and Guided Wave Letters, pp. 531-533, 2000.

(7) D. Schreurs and J. Verspecht, *"Large-signal modelling and measuring go hand-in-hand: accurate alternatives to indirect S-parameter methods,"* International Journal of RF and Microwave Computer-Aided Engineering, pp. 6-18, 2000.

(8) J. Verspecht, F. Verbeyst, M. Vanden Bossche and P. Van Esch, *"System level simulation benefits from frequency domain behavioral models of mixers and amplifiers,"* Proc. European Microwave Conference, pp. 29-32, 1999.

(9) D. Schreurs, N. Tufillaro, J. Wood, D. Usikov, L. Barford, and D.E. Root, *"Development of time domain behavioural non-linear models for microwave devices and ICs from vectorial large-signal measurements and simulations,"* Proc. European Gallium Arsenide and related III-V compounds Applications Symposium (GaAs 2000), pp. 236-239, 2000.

(10) H. Kantz and T. Schreiber, *Nonlinear Time Series Analysis*, Cambridge University Press, 1997.

(11) M. Kennel, R. Brown, and H. Abarbanel., *"Determining embedding dimension for phase-space reconstruction using a geometrical construction,"* Phys. Rev. A, pp. 3403-3411, 1992.

(12) Q.J. Zhang and K.C. Gupta, *Neural networks for RF and microwave design*, Artech House, 2000.

(13) NeuroModeler, ver. 1.2, Q. J. Zhang and his neural network research team, Department of Electronics, Carleton University, Ottawa, Canada, 1999.

(14) V. Devabhaktuni, M. Yagoub, and Q.-J. Zhang, *"A robust algorithm for automatic development of neural-network models for microwave applications,"* IEEE Trans. Microwave Theory and Techniques, Vol. 49, No. 12, pp. 2282-2291, 2001.

(15) A. Samelis and D. Pavlidis, *"Analysis of the large-signal characteristics of power heterojunction bipolar transistors exhibiting self-heating effects,"* IEEE Trans. Microwave Theory and Techniques, Vol. 45, No. 4, pp. 534-542, 1997.

(16) B. Li, S. Prasad, L.-W Yang, and S. Wang, *"Large-signal characterization of AlGaAs/GaAs HBT's,"* IEEE Trans. Microwave Theory and Techniques, Vol. 47, No. 9, pp. 1743–1746, 1999.

(17) K. Remley, J. Jargon, D. Schreurs, D. DeGroot, and K.C. Gupta, *"Repeat measurements and metrics for nonlinear model development,"* IEEE Int. Microwave Symp. Dig., pp. 2169-2172, 2002.

Table 1: Overview of the ANN training results for the SiGe HBT. Case 1: no P_{diss} included; case 2: P_{diss} included; case 3: P_{diss} included and no de-embedding of the access transmission lines.

	case 1		case 2		case 3	
	I_1	I_2	I_1	I_2	I_1	I_2
correlation	0.97810		0.99993		0.99989	
average training error	2.0%	4.5%	0.2%	0.2%	0.3%	0.3%
max. training error	32.6%	58.8%	2.7%	2.9%	3.4%	3.3%

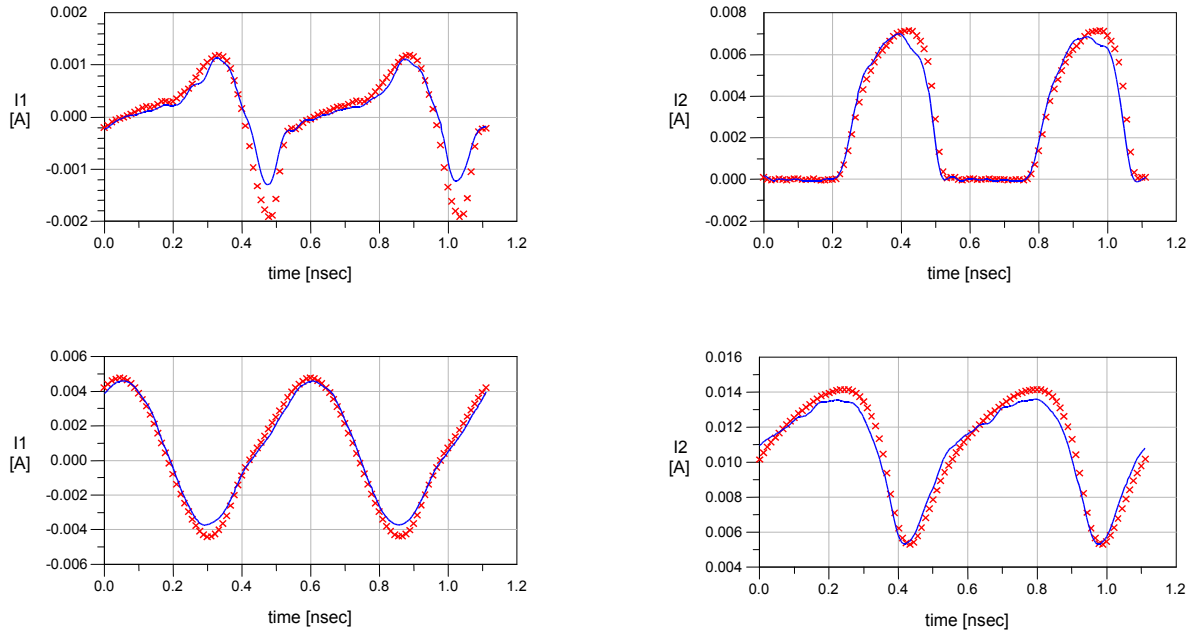

Figure 1: Comparison of the measured (x) and simulated (solid line) time domain waveforms of the terminal currents. The experimental conditions for the top plot are: V_{beDC} = 0.8 V, V_{ceDC} = 1.0 V, f_0=1.8 GHz, P_{in}= -4.4 dBm; and for the bottom plot: V_{beDC} = 1.2 V, V_{ceDC} = 1.0 V, f_0=1.8 GHz, P_{in}= -4.4 dBm.

Table 2: Metrics to quantify the model's accuracy. Conditions 1 and 2 correspond to the top and bottom plots of Fig. 1, respectively.

	Condition 1		Condition 2	
	b_1	b_2	b_1	b_2
sqrt(natural metric) [V]	1.31E-2	3.05E-2	1.81E-2	2.45E-2
weighted metric [V]	7.10E-3	1.85E-2	9.92E-3	1.22E-2